New Mexico Geological Society

Downloaded from: https://nmgs.nmt.edu/publications/guidebooks/41



Geomorphic analysis of scarps along the eastern border of the Valle Vidal, north-central New Mexico

Christopher M. Menges and James Walker
1990, pp. 431-438. https://doi.org/10.56577/FFC-41.431

in:

Tectonic Development of the Southern Sangre de Cristo Mountains, New Mexico, Bauer, P. W.; Lucas, S. G.; Mawer, C. K.; McIntosh, W. C.; [eds.], New Mexico Geological Society 41st Annual Fall Field Conference Guidebook, 450 p. https://doi.org/10.56577/FFC-41

This is one of many related papers that were included in the 1990 NMGS Fall Field Conference Guidebook.

Annual NMGS Fall Field Conference Guidebooks

Every fall since 1950, the New Mexico Geological Society (NMGS) has held an annual Fall Field Conference that explores some region of New Mexico (or surrounding states). Always well attended, these conferences provide a guidebook to participants. Besides detailed road logs, the guidebooks contain many well written, edited, and peer-reviewed geoscience papers. These books have set the national standard for geologic guidebooks and are an essential geologic reference for anyone working in or around New Mexico.

Free Downloads

NMGS has decided to make peer-reviewed papers from our Fall Field Conference guidebooks available for free download. This is in keeping with our mission of promoting interest, research, and cooperation regarding geology in New Mexico. However, guidebook sales represent a significant proportion of our operating budget. Therefore, only *research papers* are available for download. *Road logs*, *mini-papers*, and other selected content are available only in print for recent guidebooks.

Copyright Information

Publications of the New Mexico Geological Society, printed and electronic, are protected by the copyright laws of the United States. No material from the NMGS website, or printed and electronic publications, may be reprinted or redistributed without NMGS permission. Contact us for permission to reprint portions of any of our publications.

One printed copy of any materials from the NMGS website or our print and electronic publications may be made for individual use without our permission. Teachers and students may make unlimited copies for educational use. Any other use of these materials requires explicit permission.

This page is intentionally left blank to maintain order of facing pages.

GEOMORPHIC ANALYSES OF SCARPS ALONG THE EASTERN BORDER OF THE VALLE VIDAL, NORTH-CENTRAL NEW MEXICO

CHRISTOPHER M. MENGES[1] and JAMES WALKER[2]
[1]U.S. Geological Survey—Al Ain Mission, National Drilling Company, Al Ain, United Arab Emirates;
[2]Department of Geology, University of New Mexico, Albuquerque, New Mexico 87131

Abstract—A complex 3- to 5-km-long zone of west-facing topographic scarps follows the base of the steep bedrock escarpment on the northeastern border of the Valle Vidal in the eastern Sangre de Cristo Mountains of north-central New Mexico. Several possible origins may be proposed for the scarps, including: (1) surface rupture on the basin-bounding fault, (2) semi-coherent mass-wasting phenomena (e.g., earthflows or rotational slumps), or (3) relict solifluction lobes formed during earlier full-glacial climates. Several characteristics, including the general linearity of the zone, continuity across multiple drainages and topographic position in the basin, favor a tectonic origin for the scarps. The scarps occur in surficial deposits, including thin colluvial mantles on weathered bedrock and (or) steeply sloping (10°–20°) debris fans, ranging in age from late Pleistocene to late(?) Holocene, based on soil-profile development. Topographic field profiles indicate that individual scarps vary in height from 2.9 m to 22.5 m with maximum slope angles of 21.5°–31°. Graphical reconstructions from these profiles suggest possible vertical surface offsets of 1.9 m to 9 m, with the larger sizes probably related to composite (multiple-rupture) scarps. Linear regressions of log-scarp-height–maximum-slope-angle data suggest a middle to late Holocene age for the most recent rupture on these scarps; a similar rupture age is estimated from diffusion analysis of a small, probable single-event scarp. The age and size of these scarps indicate that significant Quaternary faulting and seismicity may be present in some of the intramontane valleys to the east of the central rift basins in northern New Mexico.

INTRODUCTION

The southern San Luis Valley is one of the main physiographic and structural expressions of the Rio Grande rift in northern New Mexico. This eastward-sloping basin contains a narrow deep graben bounded on the east by the major range-bounding fault zone and associated mountain front of the Sangre de Cristo Mountains (Figs. 1, 2; Upson, 1939; Dungan et al., 1984; Keller et al., 1984; Menges, 1988, 1990). The regional uplift centered over the Rio Grande rift, however, continues a considerable distance to the east across the Sangre de Cristo and Cimarron Mountains into the Raton area (Fig. 1; Cordell, 1978; Davis et al., 1984). The eastern limit of upper crustal extension and surface faulting is not well documented. It is not clear whether rift-related basins and normal faults of late Cenozoic age are confined to the central rift axis, or whether they include a discontinuous string of valleys and small basins crudely aligned along the eastern margin of the Sangre de Cristo Mountains (e.g., the Costilla–Comanche Creek valleys, the Valle Vidal, Moreno and Mora Valleys; Fig. 1). All of these north-trending intramontane valleys contain varying thicknesses of late Cenozoic sediments and are bordered on at least one side by steep, fault-bounded bedrock escarpments. In many ways the structure and morphology of these basins would appear to be small-scale analogues to the large axial rift basins to the west, which implies that the zone of active extension, surface faulting and (or) seismicity may extend farther eastward from the rift axis than is considered by most researchers.

Synchroneity of neotectonic faulting is one important element in determining the tectonic relationship between the main Rio Grande rift and the eastern border valleys described above. Many workers have documented the presence of fault scarps and other geomorphic-structural

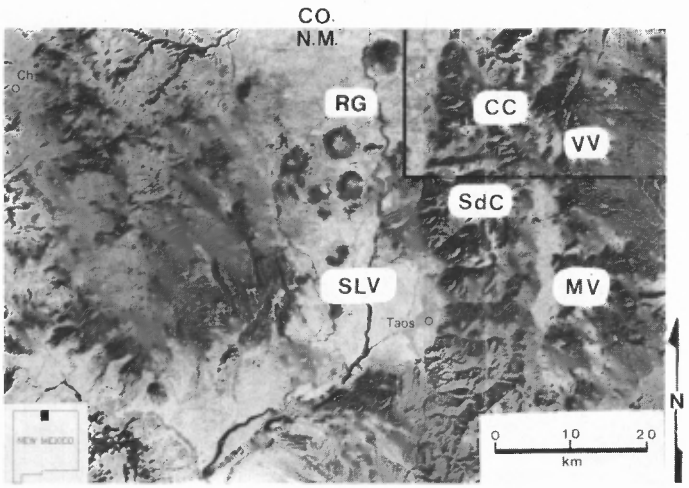


FIGURE 1. Composite Landsat image of northern Rio Grande rift near Taos and intramontane basins to the east, including the Valle Vidal study area, southern Sangre de Cristo Mountains near Taos. Solid lines in northeast corner of image outline area of Figure 2. Abbreviations are: Rio Grande gorge (RG); Sangre de Cristo Mountains (SdC); southern San Luis Valley (SLV); Valle Vidal (VV); Costilla-Comanche Creeks (CC); Moreno Valley (MV). Northern limit of map coincides with the Colorado and New Mexico border (adapted from New Mexico Geological Society, 1982).

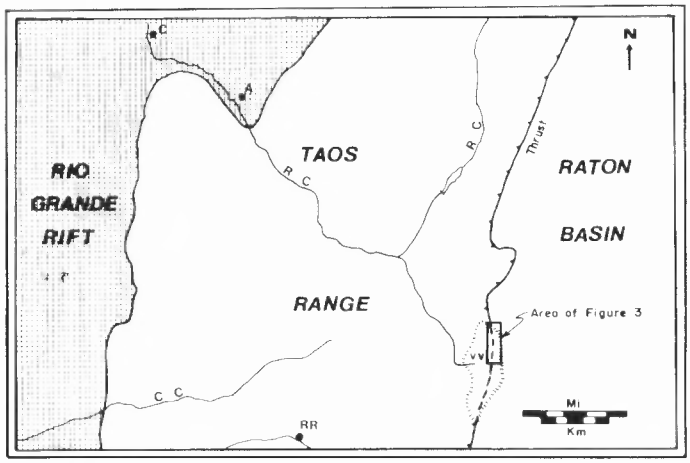


FIGURE 2. Map of Valle Vidal study area (VV) on the border between the Taos Range section of the Sangre de Cristo Mountains to the west and the Raton basin to the east. Refer to Figure 1 for a Landsat image of the physiography of this region. Symbols by category are: towns: A—Amalia, C—Costilla, RR—Red River; rivers: CC—Cabresto Creek, RC—Rio Costilla (also Costilla Creek). Barbed line indicates approximate position of large thrust-fault system on east margin of Sangre de Cristo Mountains.

indicators of Quaternary deformation in the southern San Luis Valley (Upson, 1939; Lambert, 1966; Dungan et al., 1984; Machette and Personius, 1984; Menges, 1987, 1988, 1990; Menges and Wells, 1987). However, few detailed studies of Quaternary faulting have been conducted in any of the eastern border valleys. Baltz and O'Neill (1984) suggested the possibility of Quaternary reactivation of the eastern boundary fault of the Mora Valley (see also Baltz, this volume), but reconnaissance studies by staff of the U.S. Bureau of Reclamation (unpublished report) did not find any evidence for Quaternary faulting in the upper Costilla and Moreno Valleys. Geomorphic data or analyses establishing the presence, let alone rates or amounts, of active faulting to the east of the main Rio Grande rift basins in northern New Mexico have not been reported in the literature.

Goals and scope

This paper summarizes data and morphologic analyses of an anomalous group of topographic scarps on the northeastern border of the Valle Vidal (Figs. 1, 2, 3). The morphology, stratigraphy and geomorphic position of these features suggest that they are fault scarps developed by recurrent late Quaternary surface ruptures along the eastern boundary fault of the Valle Vidal basin (see later section on scarp origins). Alternative nontectonic origins, such as slumping or solifluction, although possible, do not explain scarp characteristics as well as the surface faulting hypothesis. The ages of surface rupture potentially associated with the scarps are inferred from their morphology and relationship to late Quaternary geomorphic surfaces in the basin. Topographic profiles measured in the field across the scarps also are used to estimate paleoseismicity and recurrence intervals, assuming a tectonic origin.

STUDY AREA

The Valle Vidal is located on the physiographic and geologic boundary between the eastern edge of the Sangre de Cristo Mountains and the Raton basin (Figs. 1, 2). The latter is a dissected eastward-sloping highland on the topographic transition between the southeastern Rocky Mountains and the western Great Plains. The Raton basin corresponds geologically to a large structural and depositional trough of Laramide age containing a thick sequence of uppermost Cretaceous through Eocene sedimentary rocks locally intruded by lower to middle Tertiary stocks and dikes (Johnson and Wood, 1956; Robinson et al., 1964; Clark and Read, 1972; Baltz, 1978; Lucas and Ingersoll, 1981; Smith et al., 1985).

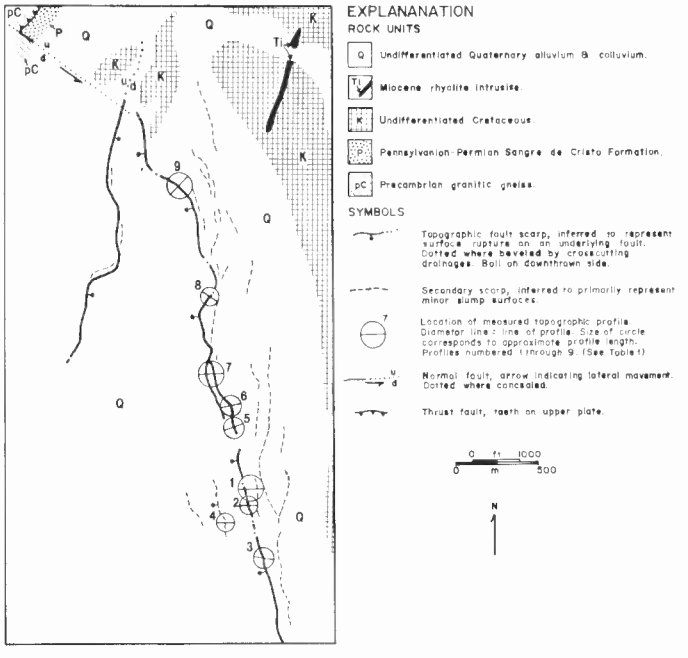


FIGURE 3. Detailed map of part of Valle Vidal, showing scarps compiled from photointerpretation and ground traverses, and the locations of measured topographic profiles of Table 1.

The western boundary of the Raton basin is defined by a complex system of west-dipping thrust and reverse faults, one strand of which projects beneath Quaternary deposits along the base of the eastern escarpment of the Valle Vidal (Figs. 2, 3). The upper plate of this thrust system is composed of Precambrian crystalline and metamorphic rocks that are widely exposed in the Taos Range of the Sangre de Cristo Mountains to the west (Clark and Read, 1972; Reed et al., 1983; Reed, 1984). This large range block reaches altitudes of 3700 m between the Valle Vidal and the southern San Luis basin in the main Rio Grande rift. The Sangre de Cristo Mountains also contain locally extensive suites of late Oligocene through Pliocene volcanic and plutonic rocks, including the silicic volcanism of the Latir volcanic field and Questa caldera, and a few Pliocene basalt flows correlated with the Taos Plateau volcanic field in the southeastern San Luis basin (Lipman and Mehnert, 1979; Lipman et al., 1986).

The Valle Vidal is a small intramontane basin, 7–8 km long and up to 3 km wide, situated at altitudes of 2900–3300 m near the regional divide between the Rio Grande and western Great Plains drainages. The cold, continental and subhumid climate of the basin (with a mean annual temperature of 2°C and a mean annual precipitation of 63 cm) supports grassland vegetation on the basin floor and ponderosa pine and juniper on the valley sideslopes (Fig. 4). The broad, undissected interior of the basin is underlain by late Quaternary alluvial fan and axial drainage deposits that overlie an unknown thickness of older Quaternary and Tertiary(?) basin fill. The low-gradient, meandering axial channel is integrated via a narrow bedrock canyon on the west-central margin of the basin with the deeply dissected valleys of Comanche and Costilla Creeks. This drainage pattern suggests relatively recent (Quaternary?) capture and integration of the interior drainage of a formerly closed structural basin by actively downcutting tributaries of the Rio Grande.

The eastern boundary of the basin is defined by a steep (15° to ≥35°) and high (200–350 m) west-facing bedrock escarpment that is much more prominent than the low dissected bedrock hills bordering the basin on the west and north. Thus the basin displays a distinct topographic asymmetry that mimics the structural geometry of an eastward-sloping half-graben, although there are no published subsurface data on the structural geometry of this basin. The bedrock of the eastern escarpment consists mainly of fractured shales near its base overlain by sandstones near the crest; these rocks are locally intruded by rhyolite dikes.

No large or deeply incised drainages have developed on the wall-like eastern escarpment; dissection is restricted to small and poorly integrated systems of rills and broad, shallow, steeply sloping valleys (Fig. 4A). A thin (<1 thick) mantle of colluvium and weathered bedrock covers the middle and lower hillslopes of the escarpment. This regolith thickens downslope into steeply inclined (15° to ≥20°) debris fans deposited along the base of the escarpment. The thickness of these undissected fans cannot be determined because their basal contacts are not exposed in the study area. The grassy hillslopes of the escarpment and basal fans are in many places disrupted by discontinuous series of small, low, arcuate scarplets (≤2–5 m in length and ≤1 m high) that have formed directly upslope from small lobes with hummocky relief. These features probably reflect the detachment and (or) downslope movement of colluvial debris as small-scale earthflows and slumps. The scarplets are much shorter in length, lower in height, and less continuous than the steep high scarps at the base of the escarpment that are the focus of this study.

METHODS

The basal scarps were mapped in detail in the field and on color aerial photographs with a nominal scale of 1:15,580 (Fig. 3). The collection and initial reduction of field data consisted of: (1) measurement of 9 topographic profiles with tape and Abney level (Figs. 3, 5; Table 1); (2) measurement of the heights and possible amounts of vertical surface displacements of scarps from field profiles (Table 1) using the graphic constructions of Machette and Personius (1984); and

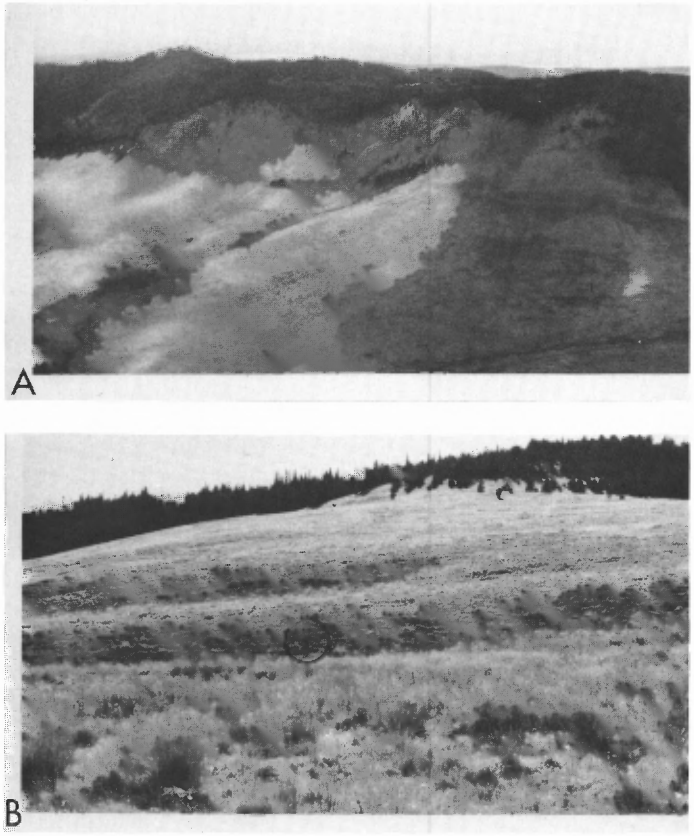


FIGURE 4. Photographs of the Valle Vidal scarps. A, aerial oblique view to east of scarps. Note complex geometry of scarps and their general linearity and continuity across several broadly defined drainages and divides on the escarpment. The scarps closely follow the contact between colluvial-mantled bedrock and alluvial debris fans along base of escarpment. B, ground view of complex set of large double scarps (VV-FS7a and b) with cumulative height of 23 m (see Fig. 5c and Table 1). Note man (circled) at base of lower scarp for scale. A few less distinct and more discontinuous scarps can be seen high on the escarpment hillslope in distance.

(3) use of three soil-profile descriptions to estimate the approximate ages of geomorphic surfaces affected by the scarps, based on correlations with several local and regional soil-geomorphic studies (McCalpin, 1982; Kelson, 1986; Wesling and McFadden, 1986; Karas, 1987; Kelson and Wells, 1987; Wesling, 1987). The age of formation of the scarps was estimated independently by two types of morphologic analysis applied to fault-scarp profiles: (1) linear regression analysis of log-scarp height versus maximum slope angle (Bucknam and Anderson, 1979; Machette and Personius, 1984) and (2) diffusion modeling of scarp-profile degradation (Nash, 1980, 1984, 1987; Colman and Watson, 1983; Hanks et al., 1984; Mayer, 1984).

SCARP CHARACTERISTICS AND MORPHOLOGY

General distribution

A complex system of west-facing topographic scarps extends 3–5 km in a north to northwest direction across alluvial and colluvial fans at the base of the northern half of the eastern escarpment (Figs. 3, 4). In plan view the scarps follow a sinuous and irregular pattern composed of numerous concave or lobate elements that commonly branch from, or overlap with, one another. In many places two to three large individual strands define a diffuse zone of multiple subparallel scarps extending from the base to midslope sections of the escarpment (Figs. 3, 4).

Zones of multiple scarps commonly contain one central element that is more continuous and linear than the others (Fig. 3). In many places this dominant strand is flanked above and below by more discontinuous

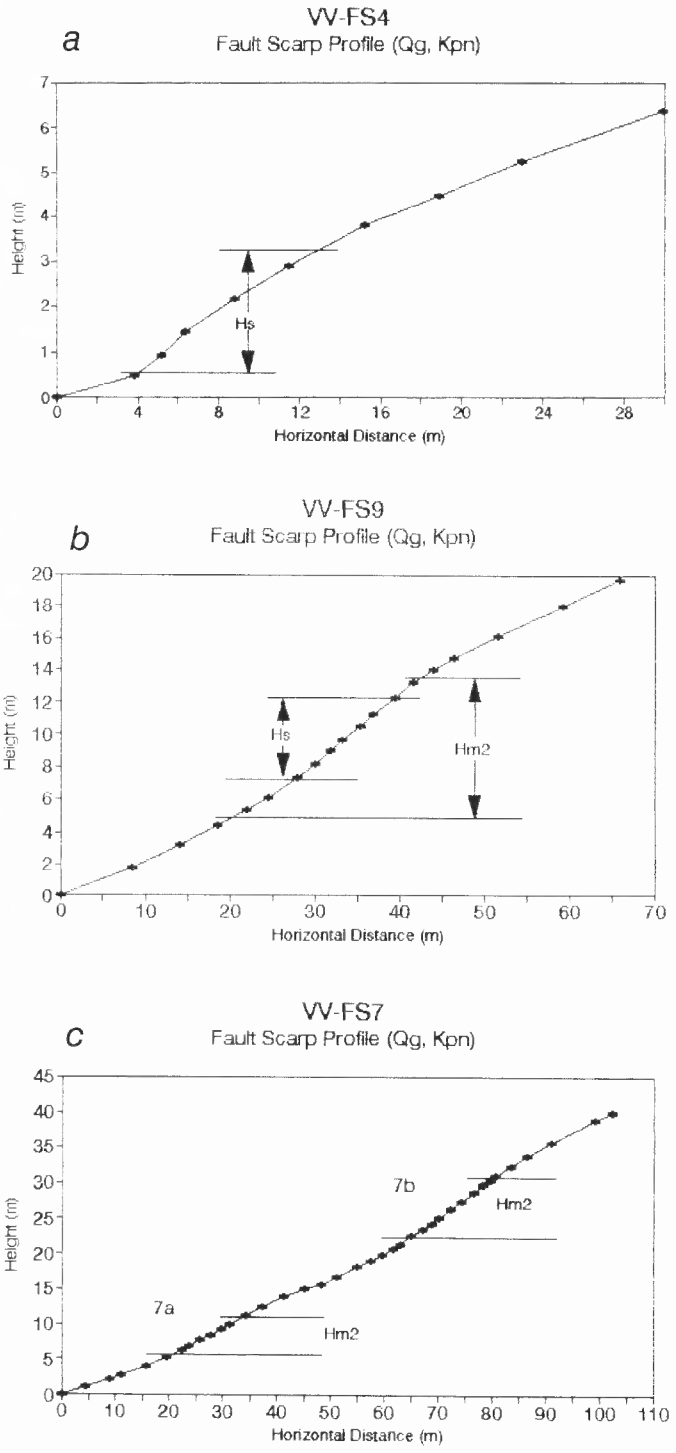


FIGURE 5. Representative topographic profiles of three different sizes and types of scarps measured in field with Abney level and tape. Tick marks indicate endpoints of measured slope sections. Hs and Hm2 indicate single-event heights and minimum composite heights of Table 1, as determined from profiles with graphical projections of Machette and Personius (1984). Refer to Figure 3 for profile locations. Profiles are plotted with different scales and vertical exaggerations. Symbols in subtitles are: Qg—Quaternary gravels; Kpn—bedrock of late Cretaceous Pierre Shales (not exposed on surface of scarps). a, profile VV-FS4, the smallest scarp measured, which is interpreted as either a single-rupture fault scarp or a related slump feature (2.3× vertical exaggeration). b, profile VV-FS9, a large single scarp, which is interpreted as composite (multiple-rupture) fault scarp (1.9× vertical exaggeration). c, profile VV-FS7, a set of large double scarps (7a and 7b), which is interpreted as zone of complex rupture on two composite fault scarps (1.3× vertical exaggeration). View from base of same scarps in Figure 4B.

TABLE 1. Tables summarizing the general characteristics and morphologies of nine field profiles measured along the Valle Vidal scarps (see Figure 3 for profile locations and Figure 5 for plots of three profiles). Alphanumeric labels for profiles (e.g., VV-FS1a, VV-FS1b) indicate lower and upper members of complex sets of scarps. Table of general characteristics and geomorphic setting of scarp profiles (above). Table of morphologic data of scarp profiles, including topographic heights, estimated offsets, maximum slope angles and slopes of original surfaces above and below scarps (below).

Profile	Scarp* Type	Geomorphic** Position	Quat.*** Surface Displaced	Aspect (deg)	Lithology****
VV-FS1a	Cp-Cm	DF	Q2	280	Qg(1a-b)
VV-FS1b	Cp(?)-Cm	DF	Q2	280	Qg(1a-b)
VV-FS2	Cp-Cm	DF	Q2	280	Qg(1e-b)
VV-FS3	Cp-Cm	Ec	Q2-1	270	Qg(1b-2a)
VV-FS4	S-Cm	P	Q3	265	Qg(1a-b)
VV-FS5	Cp-Cm	Ec	Q2-1	245	Qg(1b-2a)
VV-FS6	Cp(?)-Cm	Ec	Q1	250	Qg(1b-2a)
VV-FS7a	Cp(?)-Cm	Ec	Q1	260	Qg(1a-b)
VV-FS7b	Cp-Cm	Ec	Q1	260	Qg(1a-b)
VV-FS8	Cp(?)	OF	Q2-1	305	Qg(1a-b)
VV-FS9	Cp(?)	OF	Q2-1	250	Qg(1b-2a)

* Quat. Surfaces:
Q1 = Late - Mid. Holocene.
Q2 = Upper late Pleistocene.
Q1 = Lower(?) late Pleistocene.
Q2-1 = Late Pleistocene, Undifferentiated.

** Geomorphic Position:
P = Piedmont
OF = Debris fan, base of escarpment.
Ec = Colluvial mantle, lower escarpment.

*** Scarp Type:
S = Single rupture.
Cp = Composite
Cm = Complex

****Gravel Lithology:
Qg - Quaternary colluviel and debris fan gravels. (clast size)
1a: <0.1m
1b: 0.1-0.3m
2a: 0.3-0.5m

Profile	Composite Height (Max) Hm1 (m)	Composite Height (Min) Hm2 (m)	Single Rupture Height Hs (m)	Est. Surface Offset (Max) S1 (m)	Est. Surface Offset (Min) S2 (m)	Max. Slope Angle (Single Value) (deg)	Max. Slope Angle (Mean 10%) (deg)	Original Slope (Upper) (deg)	Original Slope (Lower) (deg)
VV-FS1a	10.0	7.0	-	5.7	2.4	30.0	29.3	15	16
VV-FS1b	-	5.7	-	2.9	0.6	28.0	25.3	15	15
VV-FS2	12.4	7.0	-	5.0	1.6	29.0	28.8	20	14
VV-FS3	22.5	17.5	-	9.0	5.6	30.0	30.0	20	17
VV-FS4	-	-	2.9	-	1.9	23.5	21.5	9	7
VV-FS5	-	7.2	4.9	3.4	1.4	25.0	24.5	14	12
VV-FS6	11.5	7.3	-	3.7	1.5	26.0	25.5	18	14
VV-FS7a	9.2	5.7	-	3.8	1.0	23.0	22.8	15	14
VV-FS7b	13.8	8.3	-	6.1	2.3	31.0	30.7	21	15
VV-FS8	-	7.3	3.3	3.7	0.9	23.0	23.0	12	12
VV-FS9	-	8.9	4.7	4.4	1.8	25.0	24.5	14	12

and arcuate scarps with similar to slightly lower heights and slope angles. The geometry of the upper set of scarps is especially discontinuous and inconsistent. This scarp system is characterized by numerous short features erratically developed on the middle and upper sections of the escarpment. The narrower zone of central and lower scarps more closely parallels the margin of the basin (Figs. 3, 4).

The scarps are developed on several different types and ages of alluvial and colluvial surfaces (Table 1). Upper Quaternary surficial deposits have not been dated radiometrically in or near the specific study area, and thus the approximate ages of geomorphic surfaces have been estimated from the associated degree of soil development. These soil correlations and age assignments are considered tentative until radiometric age control or more detailed and quantitative soil studies are available in this or adjoining areas.

Three soil profiles were described in the field on surfaces above scarps with a range of heights and morphologies. The smallest single scarp measured in the study (profile 4, Figs. 3, 5a; Table 1) is on an alluvial fan containing soils with only A and C horizons. This weakly developed soil profile (in terminology of Birkeland, 1984) suggests a probable middle to late Holocene age for the disrupted surface. The parent material has a dark mottled appearance (10 YR 3/2–3/4) and irregularly mixed textures that may be related possibly to slumping or mass-movement in this deposit.

The steep hillslopes above two higher scarps (profiles 2 and 7, Figs. 3, 5; Table 1) contain weakly to moderately developed soils exhibiting 50-cm-thick color or textural B horizons that extend through thin (50- to 100-cm-thick) layers of colluvium into weathered bedrock at shallow depths. Soil profile characteristics and thicknesses of these soils suggest probable ages of late Pleistocene to at most latest middle Pleistocene, based on comparison with soil age estimates from chronosequences in the Sangre de Cristo region (McCalpin, 1982; Kelson, 1986; Karas, 1987; Wesling, 1987, 1988; Pazzaglia, 1989). It is particularly difficult, however, to accurately assess soil ages on these steep hillslopes.

Possible scarp origins

Several tectonic and nontectonic origins may be proposed for these scarps. Many scarp characteristics suggest that they have formed by complex surface rupture along the fault zone bordering the Valle Vidal at the base of the eastern escarpment (see below). The scarps may reflect the distal margins of mass-wasting features (e.g., earthflows or rotational slumps) developed in colluvium and (or) fractured shale bedrock near the base of the steep, high escarpment. Certain features of some scarps, such as the lobate geometry and irregular hummocky terrain, particularly resemble the morphology of solifluction debris lobes that may have formed at these high altitudes during previous full glacial climates.

It is not possible to choose definitively among the various tectonic and nontectonic alternatives without trenching across the scarps. A number of scarp characteristics are more indicative of a fault-rupture origin, however, including: (1) the general linearity of the overall scarp system; (2) the lateral continuity of scarps across several different drainage systems and intervening divides on the escarpment; (3) topographic position near the transition between bedrock and basin alluvium along the base of the escarpment; (4) general absence of this type or scale of scarps elsewhere in the Valle Vidal or other adjacent intramontane basins; and (5) local development of some scarps in deposits of probable Holocene age, which post-dates the most recent glacial maximum. The presence of bedrock at shallow depths on the hillslopes above large scarps also requires that the thickness of surficial deposits be much less than the heights of scarps directly downslope. These relationships necessitate the presence of bedrock in the landslides or solifluction lobes if the scarps simply mark the downslope termination of mass-wasting features. This seems unlikely, as large detachment or pull-away zones are not evident in the escarpment above the basal scarps, and exposed bedrock on the escarpment display no obvious evidence of dislocation or transport.

The following tectonic model is considered most consistent with available data. The scarps are interpreted to have formed during complex, possibly coseismic, late Quaternary surface rupture(s) along the boundary fault. The primary zone of surface faulting probably has been concentrated on the prominent central zone of scarps. The more discontinuous upper and lower scarps in the system may reflect irregular propagation of rupture through near-surface rocks and (or) subsidiary slumping or settling of shattered bedrock during seismic shaking of the steeply sloping boundary escarpment. This process would be enhanced if the fault rupture occurred during periods of high soil and (or) moisture probably associated with full glacial conditions.

The scarps are treated as manifestations of surface faulting in subsequent geomorphic and morphologic analyses, although the other origins are considered to be feasible. The lobate shape and hummocky surface of some large, multiple-scarp systems suggest probable, locally significant modification of large pre-Holocene fault scarps by solifluction or other types of periglacial mass wasting during at least the most recent late Wisconsin glacial maximum.

Scarp heights and estimated vertical displacements

The heights and vertical surface offsets of the Valle Vidal scarps were estimated graphically from the field profiles (Fig. 5; Table 1), using the constructions of Machette and Personius (1984). Multiple sets of overlapping scarps were interpreted tectonically as complex-rupture scarps (after Mayer, 1984), although each element of the group was isolated and treated individually in morphological analyses. The total height and estimated surface offsets of the largest individual scarp (VV-FS3; Fig. 3; Table 1), however, is strikingly similar to the cumulative heights and offsets measured across a neighboring set of double scarps (VV-FS7; Figs. 3, 4B, 5C; Table 1).

The heights of individual scarps range from 2.9 m to 22.5 m (Table 1). The lowest scarp is interpreted as a probable single-rupture fault

scarp that formed during the most recent event on the main scarp system, although it may also be related in part to seismically induced slumping. Larger scarps probably represent composite fault scarps with total heights (Hm1) that reflect multiple, individual ruptures superimposed on the same fault trace. Smaller height increments (Hm2 or Hs) were defined for most composite scarps on the basis of steeper slope sections in the overall profile (Fig. 5; Table 1). Part of the Hs height component probably records the topographic signature of the most recent rupture as represented by the low, single-rupture scarp described above. Most Hs values are somewhat large, perhaps because of either difficulty in isolating the most recent event, or the tendency of the steep surrounding slopes to amplify scarp height measurements (Wallace, 1980).

Tectonic reconstructions of field profiles suggest possible surface offsets across scarps ranging from 1.9 m on the possible single-rupture scarp to a maximum of 9 m on the largest composite scarp (Table 1). Smaller displacement increments (S2) corresponding to the Hs component heights were delineated within the cumulative offset (S1) on the profiles of composite scarps. These S2 measurements average between 1.5 m and 2.0 m, depending on whether a cumulative value of S2 is summed across the multiple elements of complex scarps. Individual S2 offset increments on large scarps also are fairly similar to the displacement estimated for the possible single-rupture scarp.

The maximum slope angles of the Valle Vidal scarps are quite steep, ranging from 21.5° to 31°. The slope angles of the highest scarps approach the angle of repose of unconsolidated material. This steepness suggests a relatively young age for the scarps (see below), although in part, the high slope angles of the scarps may reflect their development in steeply sloping debris fans at the base of the bedrock escarpment. Steep ambient slopes above and below scarps tend to inflate the topographic heights of scarps in relation to the size of the original surface offset (Wallace, 1980), a factor which also explains why the estimated vertical displacements of the Valle Vidal scarps typically account for only 30%–50% of their observed heights (Table 1).

MORPHOLOGIC AGE ESTIMATES

Linear regression analyses

Figure 6 shows a graph of log scarp height (Hs) versus the maximum slope angles of the Valle Vidal scarps (Table 1), following the morphological analysis of Bucknam and Anderson (1979) as modified by Machette and Personius (1984). The general ages of undated scarps are estimated in this analysis by fitting regression lines to semi-log plots of scarp height versus maximum slope-angle data. These regressions then are compared with similar plots derived from dated reference scarps. The regression plot for the Valle Vidal scarps includes the full height of the possible single-rupture scarp (VV-FS4) combined with the heights (Hm2 or Hs) estimated from the smallest identifiable steep sections of composite scarps (Machette and Personius, 1984). The profile of the largest composite scarp (VV-FS3) was excluded from this graph because no distinct subsection of reasonable height could be isolated in this profile.

The regression-line fit to these data displays moderate correlation ($r^2 = 0.58$) with a relatively low slope and large intercept (Fig. 6). These regression line parameters probably are influenced by the large Hs heights of composite scarps relative to their slope angle. The anomalous heights reflect difficulty in clearly identifying small slope subsegments on the generally steep profiles of most of these scarps. This problem likely arises from the effects of the steep slopes of the original surfaces on the observed heights of the degraded scarps (Wallace, 1980). The height increments of many composite scarps may be too large and include one or more events pre-dating the most recent rupture, factors that commonly produce regression lines with anomalously low slopes in this type of morphologic analyses (McCalpin, 1982; Colman et al., 1985).

Regardless, all elements of the regression computed for the Valle Vidal scarps, including data points, regression line, and 95% confidence interval, lie between the reference regressions of the Fish Springs and La Jencia fault scarps with independent age control of 2 Ka and 4 Ka, respectively (Machette and Personius, 1984; Machette, 1986, 1988; Machette, written commun., 1988; Fig. 6). This relationship strongly suggests a general middle to late Holocene age for the development of the steepest sections of the Valle Vidal scarps, which corresponds to the age of the most recent rupture in tectonic interpretations.

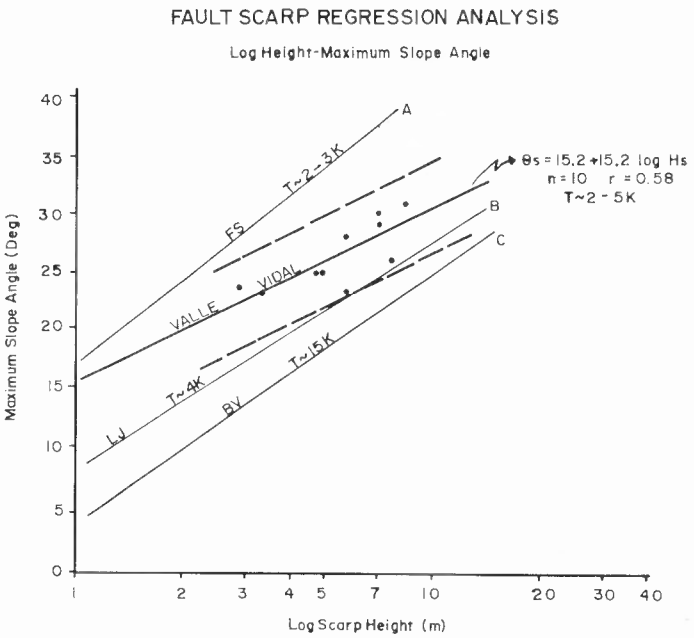


FIGURE 6. Linear regression analyses of log height vs. maximum slope angle data of Valle Vidal scarps. The smallest height increments (Hm2 or Hs) determined from field profiles were used in plotting composite scarps. Regression line fit to data is shown in heavy solid line; dashed lines indicate boundaries of 95% confidence intervals. The names and estimated ages (T, in Ka) of reference scarps with independently estimated ages are labeled in diagram. Abbreviations, location, and sources for each reference scarp are: FS—Fish Springs fault scarp, southwestern Utah, Bucknam and Anderson, 1979; Machette, written commun., 1988; LJ—La Jencia fault scarp, west-central New Mexico, Machette and Personius, 1984, and Machette, 1986, 1988; BV—Bonneville Shoreline, western Utah, Bucknam and Anderson, 1979, Machette and Personius, 1984, and Pierce and Colman, 1986.

Diffusion modeling

The diffusion modeling technique of Nash (1980, 1984, 1987a, b) was applied to profile VV-FS4. This method estimates the formation ages of topographic scarps from finite-difference solutions to a linear time-dependent diffusion equation that is used to model rates of scarp degradation. Profile VV-FS4 was chosen for analysis because it is the only scarp in the study area that reasonably satisfies the single-rupture assumption required for diffusion modeling of fault scarps (Nash, 1984).

There are two principal sources of uncertainty in this type of diffusion modeling (Menges, 1988, appendix C). First, analytical results are affected by the exact form of the initial scarp morphology assumed in diffusion modeling of subsequent scarp degradation (Nash, 1984, 1986). The numerical solution used in this study is especially sensitive to two parameters that must be specified in modeling each initial morphology. These are (1) the degree of symmetry of the initial profile about its midpoint and (2) whether the slopes of the upper and lower original surfaces (γ) are equal (parallel to one another). Several different types of initial scarp morphologies were used in modeling VV-FS4 because of the strong asymmetry in this profile (Fig. 5a).

Secondly, any diffusion technique produces a diffusion (tc) for the fault scarp, which consists of the product of time (t) since "formation" (that is, onset of diffusion-modeled degradation after surface rupture) and a diffusivity constant (c). The latter is assumed to incorporate the cumulative effects of all time-independent factors that influence the rate of scarp degradation, such as parent material, climate, vegetation, and slope aspect (Mayer, 1984, 1987; Pierce and Colman, 1986, 1987). The "constant" c may itself exhibit some dependence on the height

and initial offset of the scarp in addition to these other variables (Pierce and Colman, 1986, 1987; Pearthree et al., 1988). Past changes in climate can affect c if the scarp formed prior to the Holocene (Machette, 1986, 1988). Andrews and Hanks (1987) also indicate that the slope of the original surfaces to either side of the scarp (far-field slope) strongly affects the accuracy of the age estimate derived from diffusion modeling, although this effect is smaller for steeply sloping scarps (>22°–25°).

A model histogram technique adapted from Mayer (1984) was used to incorporate statistically these inherent analytical uncertainties into diffusion-age estimates (Fig. 7). Diffusion ages (tc) were derived from several possible initial scarp morphologies constructed for VV-FS4. Three published diffusivity constants that span an order of magnitude in scarp degradation rates (that is, c-Yellowstone from Nash, 1984; and height-corrected values of c-Idaho and c-Drum Mountain, Utah, from Pierce and Colman, 1986) were applied to each diffusion age to produce a range in age estimates for each scarp model (see Menges, 1988, appendix C for detailed description of method). The total age ranges derived for the three models of VV-FS4 were compiled together to form a composite age histogram (Fig. 7). The median and modal peak of the histogram provide general composite age estimates for this scarp profile. The histogram is distributed across a broadly defined Holocene age range, but the median (Md: 4 Ka) and modal peak (Mo: 2.5–3.5 Ka) values suggest a most probable age of middle to late Holocene, which is in good agreement with the scarp age estimated from the linear regressions of all scarp data (Figs. 6, 7).

PALEOSEISMIC INTERPRETATIONS

The magnitudes of paleoearthquakes associated with surface rupture on these scarps may be estimated from scarp morphologic data (e.g., Machette, 1986, 1988). The most recent surface-faulting event potentially associated with these scarps, assuming a tectonic origin, was probably 3–5 km long with an estimated vertical displacement of 1.5–2.0 m, although the size of the displacement seems large compared to the surface-rupture length. Surface ruptures with these characteristics would be associated with earthquakes having estimated magnitudes between 5.5–5.8 and 6.8–7.1, using the magnitude-length (M-L) and magnitude-displacement (M-D) regressions, respectively, of Slemmons (1982). The moment-magnitude relationships (Mo-M) of Hanks and Kanamori (1979) estimate earthquake magnitudes of 6.1–6.4. The results of the M-D regression appear inflated and are probably unduly influenced by poorly constrained and possibly exaggerated estimates of vertical displacements across scarps. Earthquake magnitudes derived by applying intermediate source parameters to the other two methods (M = 5.7–6.2, using L = 5 km; D = 1.5 m) are more reasonable for such a small system of scarps, and thus they are preferred as a probable upper-bound estimate for possible paleoearthquakes along this part of the Valle Vidal boundary fault.

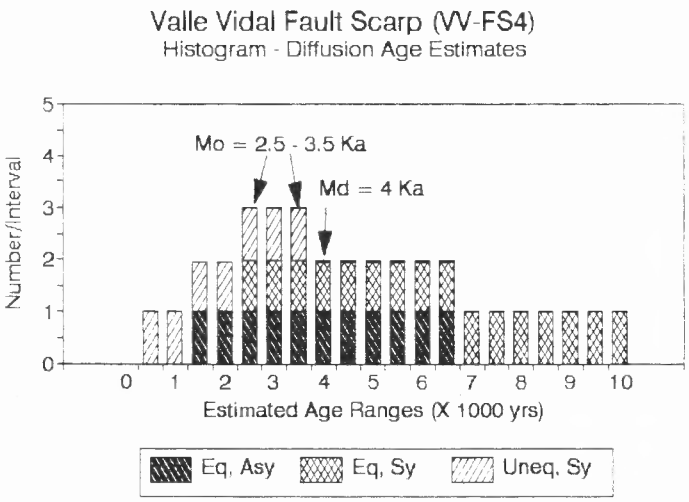


FIGURE 7. Composite age histogram of results of diffusion modeling of VV-FS4 (Fig. 5a), the only likely single-rupture scarp suitable for this type of morphologic analysis. Histogram derived from three different published diffusivity constants applied to the model results from each of three initial scarp morphologies (see text for discussion), defined in legend as equal asymmetric (Eq, Asy), equal, symmetric (Eq, Sym) and unequal, symmetric (Uneq, Sym). These terms refer to the relative slope angles of the upper and lower original surfaces and the degree of asymmetry of the initial morphology used in each model, respectively. The total number of age-range estimates that fall within 500 year class intervals are plotted as composite histograms. Mo and Md refer to age interval of the modal peak and median value in histogram, respectively.

SUMMARY AND CONCLUSIONS

A series of scarps occur along the base of the prominent bedrock escarpment that defines the northeastern margin of the Valle Vidal. A number of scarp characteristics, including linearity, continuity across drainages, topographic position and thickness and degree of soil development of associated surficial deposits, suggest that these features are probably fault scarps related to complex and irregular patterns of coseismic surface rupture on the basin-bounding fault. Several nontectonic origins are possible, however; foremost among them are development of scarps at the margins of solifluction lobes or some type of semi-coherent landslide deposits. Generally, one or two discontinuous series of scarps have formed above and below a more continuous and linear zone of central scarps at the escarpment base. This geometry is interpreted as reflecting a central zone of primary surface rupture on the boundary fault that is flanked by either seismically induced regions of slumping, or subsidiary faulting of shattered bedrock and (or) overlying surficial deposits.

Both linear regression and diffusion analysis of scarp morphology provide very similar estimates of middle to late Holocene for the youngest possible age of scarp development. This would correspond to the age of the most recent surface rupture in the fault-scarp hypothesis. These morphologic age estimates are also consistent with stratigraphic constraints on scarp age imposed by weakly developed soils of probable Holocene age observed on the youngest geomorphic surface affected by low possibly single-rupture scarps. Vertical surface offsets and rupture lengths estimated from scarp mapping and morphologic data suggest earthquakes with potential magnitudes of 5.5–7.1, and most probably between 6.1 and 6.4

The total heights and surface offsets estimated for large scarps, if tectonic, suggest that they are composite in nature. The cumulative effects of perhaps 4 to 6 individual events are inferred for the largest composite scarps by comparing their heights and surface offsets with those of the small single-rupture(?) scarp. These composite displacements of geomorphic surfaces of probable late Pleistocene age imply approximate recurrence intervals on the order of 10^3–10^4 yrs (i.e., ~5–20 Ka) for the Valle Vidal scarps.

The amount and frequency of possible late Pleistocene and younger tectonic activity on the Valle Vidal scarps are at least as high, and possibly somewhat higher, than those estimated for the range-bounding fault of the Sangre de Cristo Mountains to the west (see previous section; Menges, 1987, 1988, 1990, in press). Data on the rates and amounts of long-term faulting in the Quaternary or late Tertiary are not available for the Valle Vidal. The large vertical displacements of Pliocene basalts on the Sangre de Cristo range-front (from 500 to 1000 m in places), as well as the height of the associated mountain front, imply that cumulative post-Pliocene deformation probably is greater on the Sangre de Cristo fault (op. cit.; also Menges and Wells, 1987). Nevertheless, the presence of possible late Quaternary fault scarps of the size proposed in this study strongly suggests that locally significant Quaternary extensional deformation may be occurring on the boundary faults of at least some of the intramontane basins on the eastern flank of the Rio Grande rift in northern New Mexico.

ACKNOWLEDGMENTS

This study was conducted as part of dissertation research by Menges on the tectonic geomorphology of the western mountain front of the Sangre de Cristo Mountains, which received partial financial support from the following funding sources: a Challenge Scholarship grant from

the Office of Graduate Studies at the University of New Mexico; funds provided by the New Mexico Bureau of Mines and Mineral Resources; the 1986 New Mexico Geological Society Fellowship; and a 1986 Mackin and general grant-in-aid from the Geological Society of America. Menges also received financial support from the U.S. Bureau of Reclamation during data analysis and manuscript preparation. Reviews by J. C. Dohrenwend, M. Pavich and M. J. Bergin greatly improved the quality of this manuscript.

REFERENCES

Baltz, E. H., 1978, Resume of Rio Grande depression in north-central New Mexico; *in* Hawley, J. W., ed., Guidebook to the Rio Grande rift in New Mexico and Colorado: New Mexico Bureau of Mines and Mineral Resources, Circular 163, pp. 210–228.

Baltz, E. H. and O'Neill, J. M., 1984, Geologic map and cross-sections of the Mora River area, Sangre de Cristo Mountains, Mora County, New Mexico: U.S. Geological Survey, Miscellaneous Investigations Map I-1456, scale 1:24,000.

Birkeland, P. W., 1984, Soils and geomorphology: New York and Oxford, Oxford University Press, 372 pp.

Bucknam, R. C. and Anderson, R. E., 1979, Estimation of fault-scarp ages from a scarp-height–slope-angle relationship: Geology, v. 7, pp. 11–14.

Clark, K. F. and Read, C. B., 1972, Geology and ore deposits of Eagle Nest area, New Mexico Bureau of Mines and Mineral Resources, Bulletin 94, 152 pp.

Colman, S. M., McCalpin, J. P., Ostenaa, D. A. and Kirkham, R. M., 1985, Map showing upper Cenozoic rocks and deposits and Quaternary faults, Rio Grande rift, south-central Colorado: U.S. Geological Survey, Miscellaneous Investigations Map I-1594, scale 1:125,000.

Colman, S. M. and Watson, K., 1983, Ages estimated from a diffusion equation model for scarp degradation: Science, v. 221, pp. 263–265.

Cordell, L., 1978, Regional geophysical setting of the Rio Grande rift: Geological Society of America Bulletin, v. 89, pp. 1073–1090.

Davis, P. M., Parker, E. C., Evans, J. R., Iyer, H. M. and Olsen, K. H., 1984, Teleseismic deep sounding of the velocity structure beneath the Rio Grande rift: New Mexico Geological Society, Guidebook 35, pp. 29–38.

Dungan, M. A., Muehlberger, W. R., Leininger, L., Peterson, C., McMillan, N. J., Gunn, G., Lindstrom, M. and Haskin, L., 1984, Volcanic and sedimentary stratigraphy of the Rio Grande gorge and the late Cenozoic geologic evolution of the southern San Luis Valley: New Mexico Geological Society, Guidebook 35, pp. 157–170.

Hanks, T. C. and Andrews, D. J., 1987, Far-field slopes and the nature of general diffusion models of scarplike landforms in weakly consolidated materials; *in* Crone, A. J. and Omdahl, E. M., eds., Proceedings of conference XXXIX—directions in paleoseismology: U.S. Geological Survey, Open-file Report 87-673, pp. 339–355.

Hanks, T. C., Bucknam, R. C., Lajoie, K. R. and Wallace, R. E., 1984, Modification of wave-cut and faulting-controlled landforms: Journal of Geophysical Research, v. 89, pp. 5771–5790.

Hanks, T. C. and Kanamori, Hiroo, 1979, A moment magnitude scale: Journal of Geophysical Research, v. 84, pp. 2348–2350.

Johnson, R. B. and Wood, G. H., 1956, Stratigraphy of Upper Cretaceous and Tertiary rocks of Raton basin, Colorado and New Mexico: American Association of Petroleum Geologists Bulletin, v. 40, pp. 707–721.

Karas, P. A., 1987, Quaternary alluvial sequence of the upper Pecos River and a tributary, Glorieta Creek, north-central New Mexico; *in* Menges, C. M., Enzel, Y. and Harrison, B., eds., Friends of the Pleistocene—Rocky Mountain cell, fieldtrip guidebook, pp. 159–176.

Keller, G. R., Cordell, L., Davis, G. H., Peeples, V. J. and White, G., 1984, A geophysical study of the San Luis basin: New Mexico Geological Society, Guidebook 35, pp. 51–57.

Kelson, K. I., 1986, Long-term tributary adjustments to base-level lowering, northern Rio Grande rift, New Mexico [M.S. thesis]: Albuquerque, University of New Mexico, 211 pp.

Kelson, K. I. and Wells, S. G., 1987, Present-day fluvial hydrology and long-term tributary adjustments, northern New Mexico; *in* Menges, C. M., Enzel, Y. and Harrison, B., eds., Friends of the Pleistocene—Rocky Mountain cell, fieldtrip guidebook, pp. 95–109.

Lambert, P. W., 1966, Notes on the late Cenozoic geology of the Taos-Questa area, New Mexico: New Mexico Geological Society, Guidebook 17, pp. 43–50.

Lipman, P. W. and Mehnert, H. H., 1979, The Taos Plateau volcanic field, northern Rio Grande rift, New Mexico; *in* Reicker, R. E., ed., Rio Grande rift: tectonics and magmatism: Washington, D.C., American Geophysical Union, pp. 289–311.

Lipman, P. W., Mehnert, H. H. and Naeser, C. W., 1986, Evolution of the Latir volcanic field, northern New Mexico, and its relation to the Rio Grande rift, as indicated by potassium-argon and fission track dating: Journal of Geophysical Research, v. 91, pp. 6329–6345.

Lucas, S. G. and Ingersoll, R. V., 1981, Cenozoic continental deposits of New Mexico: an overview: Geological Society of America Bulletin, v. 92, pp. 917–932.

Machette, M. N., 1986, History of Quaternary offset and paleoseismicity along the La Jencia fault, central Rio Grande rift, New Mexico: Bulletin of the Seismological Society of America, v. 76, pp. 259–272.

Machette, M. N., 1988, Quaternary movement along the La Jencia fault, New Mexico: U.S. Geological Survey, Professional Paper 1440, 82 pp.

Machette, M. N. and Personius, S. F., 1984, Map of Quaternary and Pliocene faults in the eastern part of the Aztec 1° × 2° quadrangle and the western part of the Raton 1° × 2° quadrangle, northern New Mexico: U.S. Geological Survey, Miscellaneous Field Studies Map MF-1465-B, scale 1:250,000 with text, 20 pp.

Mayer, L., 1984, Dating Quaternary fault scarps formed in alluvium using morphologic parameters: Quaternary Research, v. 22, pp. 300–313.

Mayer, L., 1987, Sources of error in morphologic dating of fault scarps; *in* Crone, A. J. and Omdahl, E. M., eds., Proceedings of conference XXXIX—directions in paleoseismology: U.S. Geological Survey, Open-file Report 87-673, pp. 302–310.

McCalpin, J. P., 1982, Quaternary geology and neotectonics of the west flank of the northern Sangre de Cristo Mountains, south-central Colorado: Colorado School of Mines Quarterly, v. 77, 97 pp.

Menges, C. M., 1987, Temporal and spatial segmentation of Pliocene-Quaternary fault rupture along the western Sangre de Cristo mountain front, northern New Mexico; *in* Crone, A. J. and Omdahl, E. M., eds., Proceedings of conference XXXIX—directions in paleoseismology, U.S. Geological Survey, Open-file Report 87-673, pp. 203–222.

Menges, C. M., 1988, The tectonic geomorphology of mountain-front landforms in the northern Rio Grande rift near Taos, New Mexico [Ph.D. dissertation]: Albuquerque, University of New Mexico, 339 pp.

Menges, C. M., 1990, Late Cenozoic rift tectonics and mountain-front landforms of the Sangre de Cristo Mountains near Taos, northern New Mexico: New Mexico Geological Society, Guidebook 41.

Menges, C. M., in press, Late Cenozoic fault scarps, mountain-front landforms, and Pliocene-Quaternary segmentation of the range-bounding fault zone, Sangre de Cristo Mountains, New Mexico; *in* Krinitzsky, E. L. and Slemmons, D. B., eds., Neotectonics in earthquake evaluation, reviews in engineering geology, v. 8: Geological Society of America, Special Paper.

Menges, C. M. and Wells, S. G., 1987, Late Quaternary fault scarps, mountain front landforms, and Plio-Quaternary rupture segmentation along a range-front normal fault zone, Sangre de Cristo Mountains, New Mexico: Geological Society of America, Abstracts with Programs, v. 19, pp. 770–771.

Nash, D. B., 1980, Morphologic dating of the degraded normal fault scarps: Journal of Geology, v. 89, pp. 353–360.

Nash, D. B., 1984, Morphologic dating of fluvial terrace scarps and fault scarps near West Yellowstone, Montana: Geological Society of America Bulletin, v. 95, pp. 1413–1424.

Nash, D. B., 1986, Morphologic dating and modeling degradation of fault scarps; *in* Active tectonics, studies in geophysics: Washington, D.C., National Academy Press, pp. 181–194.

Nash, D. B., 1987a, SLOPEAGE program, v. 2.1: Fenneman-Rich Geomorphic Laboratories: Department of Geology, University of Cincinnati, Cincinnati, OH 45221-0013.

Nash, D. B., 1987b, Reevaluation of the linear-diffusion model for morphologic dating of scarps; *in* Crone, A. J. and Omdahl, E. M., eds., Proceedings of conference XXIX—directions in paleoseismology: U.S. Geological Survey, Open-file Report 87-673, pp. 325–338.

New Mexico Geological Society, 1982, New Mexico highway geologic map: Socorro, New Mexico Geological Society, scale 1:1,000,000.

Pazzaglia, F. J., 1989, Tectonic and climatic influences on the evolution of Quaternary depositional landforms along a segmented range-front fault, Sangre de Cristo Mountains, north-central New Mexico [M.S. thesis]: Albuquerque, University of New Mexico, 246 pp.

Pearthree, P. A., Demsey, K. A., Fonseca, J. and Hecker, S., 1988, An evaluation of morphologic analysis of pluvial shoreline scarps and young fault scarps in central Nevada: Geological Society of America, Abstracts with Programs, v. 20, pp. 220–221.

Pierce, K. L. and Colman, S. M., 1986, Effect of height and orientation (microclimate) on geomorphic degradation rates and processes, late-glacial terrace scarps in central Idaho: Geological Society of America Bulletin, v. 97, pp. 869–885.

Reed, J. C., Jr., 1984, Proterozoic rocks of the Taos Range, Sangre de Cristo

Mountains, New Mexico: New Mexico Geological Society, Guidebook 35, pp. 179–185.
Reed, J. C., Lipman, P. W. and Robertson, J. E., 1983, Geologic map of the Latir Peak and Wheeler Peak Wilderness and Columbine-Hondo Wilderness Study Area, Taos County, New Mexico: U.S. Geological Survey, Miscellaneous Field Studies Map MF-1570-B, scale 1:50,000.
Robinson, G. D., Wanek, A. A., Hays, W. H. and McCallum, M. E., 1964, Philmont country—the rocks and landscape of a famous New Mexico ranch: U.S. Geological Survey, Professional Paper 505, 152 pp.
Slemmons, D. B., 1982, Determination of design earthquake magnitudes for microzonation: Proceedings of the Third International Earthquake Microzonation Conference, v. 1, pp. 119–130.
Smith, L. N., Lucas, S. G. and Elston, W. E., 1985, Paleogene stratigraphy, sedimentation, and volcanism of New Mexico; *in* Flores, R. M. and Kaplan, W. D., eds., Cenozoic paleogeography of the west-central United States: Denver, Rocky Mountain Section, Society of Economic Paleontologists and Mineralogists, pp. 293–316.
Upson, J. E., 1939, Physiographic subdivisions of the San Luis Valley, southern Colorado: Journal of Geology, v. 47, pp. 721–736.
Wallace, R. E., 1980, Discussion—nomograms for estimating components of fault displacement from measured height of fault scarp: Bulletin of the Association of Engineering Geologists, v. 17, pp. 39–45.
Wesling, J. R., 1987, Glacial chronology of Winsor Creek drainage basin, Sangre de Cristo Mountains, New Mexico; *in* Menges, C. M., Enzel, Y. and Harrison, B., eds., Friends of the Pleistocene—Rocky Mountain cell, fieldtrip guidebook, pp. 177–190a.
Wesling, J. R., 1988, Glacial chronology and soil development in Winsor Creek drainage basin, southernmost Sangre de Cristo Mountains, New Mexico [M.S. thesis]: Albuquerque, University of New Mexico, 186 pp.
Wesling, J. R. and McFadden, L. D., 1986, Pleistocene and Holocene glacial chronology for the glacial deposits in the southernmost Sangre de Cristo Mountains, New Mexico: Geological Society of America, Abstracts with Programs, v. 18, p. 422.



Baldy Deep Tunnel Mine on Baldy Mountain, circa 1915. Photo by Thomas Fitzsimmons; courtesy of Museum of New Mexico, neg. no. 30551.